

# Weighting Function Integrated in Grid-interfacing Converters for Unbalanced Voltage Correction

Fei Wang, Jorge L. Duarte, Marcel A. M. Hendrix

Department of Electrical Engineering  
Eindhoven University of Technology  
5600 MB Eindhoven, The Netherlands

Phone number: +0031 40 2473566, e-mail: f.wang@tue.nl

**Abstract.** In this paper a weighting function for voltage unbalance correction is proposed to be integrated into the control of distributed grid-interfacing systems. The correction action can help decrease the negative-sequence voltage at the point of connection with the grid. Based on the voltage unbalance factor and system power capacity, the interfacing converter delivers a small amount of negative-sequence current to the grid and helps correcting the negative-sequence voltage. Although the reduced amplitudes contributed by each individual DG system are very small compared to the total negative-sequence component, many DG system modules can collectively achieve substantial results in the grid. As a practical example, a three-phase grid-interfacing converter servicing sensitive loads with distributed sources is employed to integrate this additional function. Design principles, simulation and experimental results are presented to verify the proposal.

## Key words

Weighting function, unbalanced voltage, grid-interfacing converter, power quality, distributed generation.

## 1. Introduction

For three-phase power systems, the voltages are expected to be sinusoidal and balanced. However, voltage unbalance problems exist in a practical utility grid. Major causes are the unbalanced distribution of single-phase loads and nonlinear loads which cause unequal voltage drops in the transformer and line impedances. Zero-sequence components do not exist in three-wire systems. But negative-sequence voltages are especially troublesome. The effects of voltage unbalance problems are quite severe for electrical machines, power electronic converters, and drives [1].

Active compensators are especially applied for voltage unbalance mitigation of the utility grid by regulating reactive power or, to maintain a balanced voltage at the load terminals, by injecting series compensated voltages [2]-[6]. These compensators are normally applied to improve the problems mainly at high voltage levels.

Over the years, many grid-interfacing systems have been studied for better performance in various grid situations. The interfacing electronic converters mainly focus on the

control of the current quality based on harmonic standards. For the unbalanced situation, techniques have been proposed to mitigate the negative-sequence and zero-sequence currents, in order to protect grid-connected equipment from voltage unbalance problems [7]-[10]. However, the techniques do not manage to correct the voltage unbalance of the grid coming from the distribution end.

Analogous to the obliged harmonic limitation for electricity loads, negligible harmonic fractions that are limited for each individual load can collectively be significant to the whole utility grid. If the negative-sequence currents are generated by each grid-interfacing converter system to help correcting negative-sequence voltages, the objective of eliminating negative-sequence voltages at the point of connection (POC) with the grid may be achieved. Each individual system can perform compensation automatically based on its own power capacity and the particular situation of the grid voltage at the POC. In this way, the negative-sequence grid voltage is corrected incrementally. The more of these correction modules are connected, the more the unbalance is suppressed.

This paper introduces the concept of negative-sequence voltage correction by grid-interfacing systems at the low voltage level. Each of the system modules helps to decrease the negative-sequence voltage by delivering a small amount of negative-sequence current into the grid, based on the voltage unbalance factor (VUF) [1]. The correction principle is analyzed for single and multiple modules. Possible application fields are presented. Finally, a three-phase grid-interfacing system for power quality improvement is used to test this additional functionality. The control scheme is analytically studied. Simulation and experimental results are presented to verify the control strategy and system performance.

## 2. Voltage Unbalance Correction

### A. Negative-sequence Equivalent Model

For the analysis of negative-sequence components, an equivalent model is derived in the following. Fig. 1

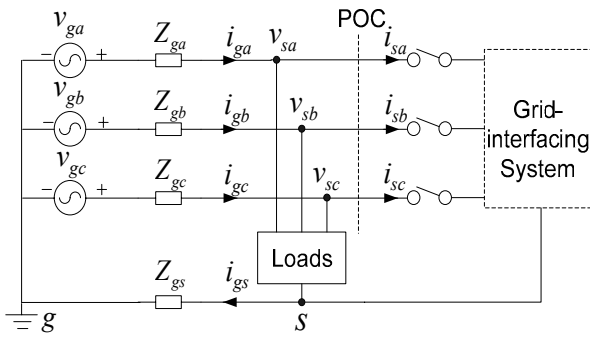


Fig. 1. Grid-interfacing system at POC.

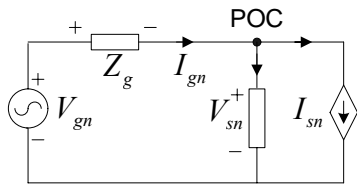


Fig. 2. Equivalent model for the negative-sequence component.

shows the structure of a three-phase four-wire grid-interfacing system being connected to the utility grid at the POC. Some other loads are also present at the POC.

With the theory of symmetric decomposition for three phase systems, the unbalanced grid voltages can be divided into three groups of balanced voltages, namely positive-sequence, negative-sequence and zero-sequence. Currents can be separated similarly. In the following, the subscripts “p”, “n” and “z” denote the positive, negative and zero sequences, respectively. The impedances of each line are given as  $Z_{ga}$  to  $Z_{gs}$ , as illustrated in the diagram. (The mutual impedances between the phases are not taken into account.) In phasor notation the grid voltages can be expressed by

$$\begin{bmatrix} \underline{V}_{-ga} \\ \underline{V}_{-gb} \\ \underline{V}_{-gc} \end{bmatrix} = \underline{Z} \begin{bmatrix} \underline{I}_{ga} \\ \underline{I}_{gb} \\ \underline{I}_{gc} \end{bmatrix} + \underline{Z}_{gs} \begin{bmatrix} \underline{I}_{gs} \\ \underline{I}_{gs} \\ \underline{I}_{gs} \end{bmatrix} + \begin{bmatrix} \underline{V}_{-sa} \\ \underline{V}_{-sb} \\ \underline{V}_{-sc} \end{bmatrix}, \quad (1)$$

where

$$\underline{Z} = \begin{bmatrix} \underline{Z}_{ga} & 0 & 0 \\ 0 & \underline{Z}_{gb} & 0 \\ 0 & 0 & \underline{Z}_{gc} \end{bmatrix}. \quad (2)$$

Based on the theory of symmetric decomposition for unbalance system [11], the power invariant transformation of quantities from p-n-z to a-b-c components are

$$\begin{bmatrix} \underline{V}_{-ga} \\ \underline{V}_{-gb} \\ \underline{V}_{-gc} \end{bmatrix} = \underline{A} \begin{bmatrix} \underline{V}_{-gz} \\ \underline{V}_{-gp} \\ \underline{V}_{-gn} \end{bmatrix}, \quad \begin{bmatrix} \underline{I}_{ga} \\ \underline{I}_{gb} \\ \underline{I}_{gc} \end{bmatrix} = \underline{A} \begin{bmatrix} \underline{I}_{gz} \\ \underline{I}_{gp} \\ \underline{I}_{gn} \end{bmatrix}, \quad (3)$$

$$\begin{bmatrix} \underline{V}_{-sa} \\ \underline{V}_{-sb} \\ \underline{V}_{-sc} \end{bmatrix} = \underline{A} \begin{bmatrix} \underline{V}_{-sz} \\ \underline{V}_{-sp} \\ \underline{V}_{-sn} \end{bmatrix}, \quad (4)$$

where

$$\underline{A} = \frac{1}{3} \begin{bmatrix} 1 & 1 & 1 \\ 1 & a & a^2 \\ 1 & a^2 & a \end{bmatrix}, \quad a = e^{-j\frac{2\pi}{3}}. \quad (5)$$

Furthermore, the neutral current is calculated to be

$$\underline{I}_{gs} = \underline{I}_{ga} + \underline{I}_{gb} + \underline{I}_{gc} = 3\underline{I}_{gz}. \quad (6)$$

Substituting (3), (4) and (6) into (1) yields

$$\underline{A} \begin{bmatrix} \underline{V}_{-gz} \\ \underline{V}_{-gp} \\ \underline{V}_{-gn} \end{bmatrix} = \underline{Z} \underline{A} \begin{bmatrix} \underline{I}_{gz} \\ \underline{I}_{gp} \\ \underline{I}_{gn} \end{bmatrix} + \underline{Z}_{gs} 3 \begin{bmatrix} \underline{I}_{gz} \\ \underline{I}_{gz} \\ \underline{I}_{gz} \end{bmatrix} + \underline{A} \begin{bmatrix} \underline{V}_{-sz} \\ \underline{V}_{-sp} \\ \underline{V}_{-sn} \end{bmatrix}. \quad (7)$$

For simplicity, it is assumed that the impedances of the utility grid are the same for each phase, that is  $\underline{Z}_{ga} = \underline{Z}_{gb} = \underline{Z}_{gc} = \underline{Z}_g$ . By multiplying with  $\underline{A}^{-1}$ , equation (7) can be rewritten as

$$\begin{bmatrix} \underline{V}_{-gz} \\ \underline{V}_{-gp} \\ \underline{V}_{-gn} \end{bmatrix} = \underline{Z}_g \begin{bmatrix} \underline{I}_{gz} \\ \underline{I}_{gp} \\ \underline{I}_{gn} \end{bmatrix} + 3\underline{Z}_{gs} \begin{bmatrix} \underline{I}_{gz} \\ 0 \\ 0 \end{bmatrix} + \begin{bmatrix} \underline{V}_{-sz} \\ \underline{V}_{-sp} \\ \underline{V}_{-sn} \end{bmatrix}. \quad (8)$$

According to (8), the equivalent impedances for positive, negative and zero sequences are decoupled. Both positive and negative sequences have the same impedance  $\underline{Z}_g$ .

Then an equivalent circuit model for sequence voltages can be derived. The diagram for negative-sequence components is shown in Fig. 2. Voltage  $\underline{V}_{gn}$  and  $\underline{V}_{sn}$  are the negative-sequence voltages of the utility grid and POC, respectively. Current  $\underline{I}_{sn}$  is the negative-sequence current from the grid-interfacing system.

### B. Negative-sequence Voltage Correction

The idea is to induce controllable voltage on the grid impedances by regulating the negative-sequence component of the current flowing between the system and the grid. Consequently, the voltage  $\underline{V}_{sn}$  is corrected by the negative-sequence voltage drop on the grid impedance.

Concerning the impedance  $\underline{Z}_g$ , this is a combination of inductance and resistance. E.g., for overhead lines, the ratio of resistance to inductance R/X is almost 1, and is about 4~5 for some underground cables. The proposed method can be effective in both situations, while the conventional reactive power correction method is hardly useful for cables. Thus a general situation is analyzed for

$$\underline{Z}_g = Z_g \angle \varphi. \quad (9)$$

The negative-sequence current is controlled to follow the same fundamental frequency of the grid voltage. Taking

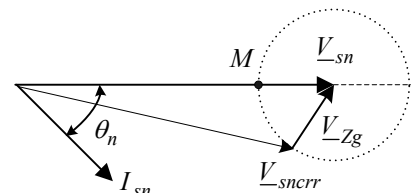


Fig. 3. Phasor diagram of the negative-sequence voltage

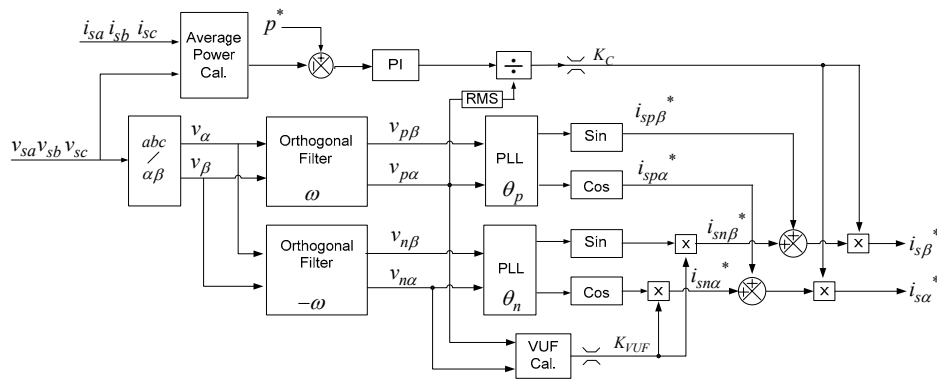


Fig. 5. Block diagram of current reference generation for the series inverter control.

$\underline{V}_{sn}$  as phase reference, that is  $\underline{V}_{sn} = V_{sn} \angle 0^\circ$ , current  $\underline{I}_{sn}$  is expressed as

$$\underline{I}_{sn} = I_{sn} \angle \theta_n. \quad (10)$$

Fig. 3 shows a phasor diagram where the negative-sequence current is controlled. The phasor  $\underline{V}_{sn}$  indicates the initial value before correction.  $\theta_n$  denotes the phase angle between negative-sequence voltage and current. By changing the amplitude and phase of the negative-sequence current  $I_{sn}$ , the initial voltage is regulated to  $\underline{V}_{snerr}$  at the POC. For a certain amplitude  $I_{sn}$ , the voltage changes along the dashed circle and reaches minimum value at the point  $M$  when  $\theta_n$  equals  $-\varphi$ .

Considering that this correction function is independently controlled for the negative-sequence current, it is feasible to integrate this additional functionality into a grid-interfacing system which has already achieved positive-sequence current control when the grid voltage is unbalanced. Therefore, the key points for voltage correction are the generation of reference signals and their implementation. A practical application is presented in the next section. Similarly, this idea can also be applied to other line current controlled systems, such as an active power filter, where it can be combined with harmonic compensation.

### 3. Practical Application

#### A. Set-up Configuration

Fig. 4 shows a three-phase four-wire grid-interfacing system, which is designed to deliver bidirectional power with distributed sources. It consists of two four-leg inverters, one in parallel and the other in series with the grid. A common DC-link is supplied by distributed sources which output electricity in DC form [12].

The parallel inverter operates as a voltage source to maintain balanced and sinusoidal voltages for the local sensitive loads. The series converter is used to handle bidirectional power flow and power quality of the line currents. A four-leg full bridge topology is used for the mitigation of zero-sequence currents. The flexible experimental set-up in Fig. 4 can be used to integrate the proposed additional feature of negative-sequence voltage correction into the original control.

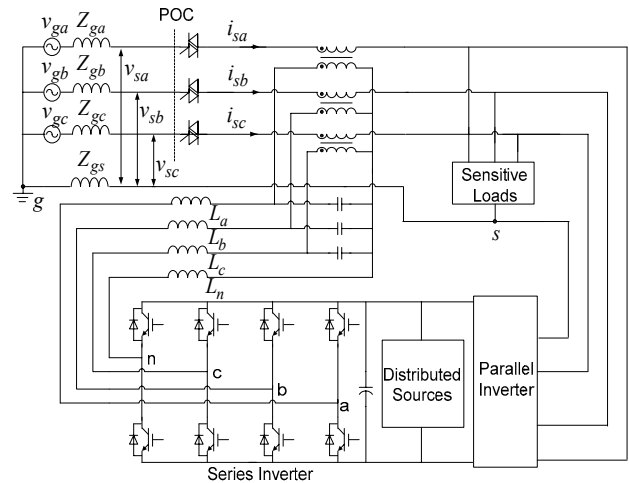


Fig. 4. Three-phase four-wire grid-interfacing system.

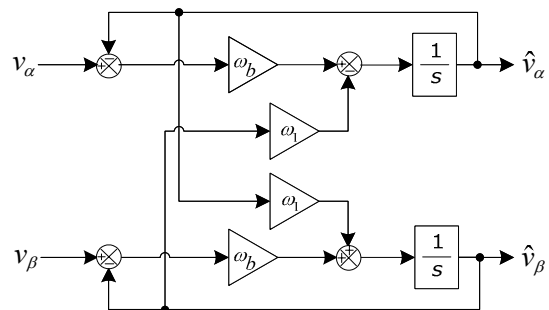


Fig. 6. Block diagram of the band-pass filter.

#### B. Control Scheme

The control of the whole system will not be presented here because only the control of the series inverter has to be modified. The emphasis in this paper is giving an example on how to generate the desired new current references instead of the original set that only contains fundamental positive-sequence currents.

Fig. 5 shows a block diagram of the reference current generation for the series inverter. This control block consists of the separation of sequence voltages, PLL, average power control and the synthesis of signals.

Considering unbalanced and distorted grid voltages, a filter with good performance is needed to filter out the

fundamental positive-sequence and negative-sequence components accurately. The separation of the sequence voltages is achieved by two orthogonal filters. Fig. 6 shows the inner structure of the employed filter that is designed to derive positive-sequence voltages [13]. Both the input and output are quantities in the  $\alpha$ - $\beta$  stationary frame. The mathematical presentation of the filter is

$$\begin{aligned} \hat{v}_\alpha(s) &= \frac{1}{s} [\omega_p (v_\alpha(s) - \hat{v}_\alpha(s)) - \omega_1 \hat{v}_\beta(s)] \\ \hat{v}_\beta(s) &= \frac{1}{s} [j\omega_p (v_\beta(s) - \hat{v}_\beta(s)) + \omega_1 \hat{v}_\alpha(s)]. \end{aligned} \quad (11)$$

The quantities of the  $\alpha$ - $\beta$  frame can be assumed to be orthogonal complex numbers. Thereby Eq. (11) can also be rewritten as a transfer function for complex variables.

$$\frac{\hat{v}_\alpha(s) + j\hat{v}_\beta(s)}{v_\alpha(s) + jv_\beta(s)} = \frac{\omega_b((s + \omega_b) + j\omega_1)}{(s + \omega_b)^2 + \omega_1^2}. \quad (12)$$

So (12) can be interpreted as a band-pass filter in the stationary frame. The parameter  $\omega_b$  is half the passing band and  $\omega_1$  is the central frequency. By defining the central frequency  $\omega_1$  as the fundamental frequency of the grid voltage  $\omega$  or  $-\omega$ , the positive-sequence and negative-sequence components can be derived in the  $\alpha$ - $\beta$  frame separately, as illustrated in Fig. 5. Note that, under the situation of very small fraction for negative-sequence component, two orthogonal filters can be used in cascade to get more accurate results.

The synthesis of phases and amplitudes are achieved by two phase-locked loops (PLL), the  $VUF$  calculation and average power control. The PLL employs a conventional control method with PI controllers for three-phase systems. Since the input  $\alpha$ - $\beta$  signals for PLL, output by the orthogonal filters, are always clean and orthogonal sinusoidal waveforms, the PLLs can have good phase tracking even under unbalanced or distorted grid voltages. For the positive-sequence components, it is designed to be always in phase or inverse with the grid voltage in order to deliver only active power. Thus,  $\theta_p$  which denotes the phase angle between positive-sequence voltage and current is zero or  $\pi$ . As discussed in the previous section, the phase-shift  $\theta_n$  of the negative-sequence current component is set to equal  $-\varphi$  for a maximum correction effect.

The  $VUF$  ratio denoted by  $K_{VUF}$ , that is the ratio between the amplitude of the negative-sequence voltage and the amplitude of the positive-sequence voltage at the POC, is used to determine the weights of the two sequence currents. In this case, a constraint equation is proposed to calculate the desired amplitude of the negative-sequence current  $I_{sn}$ . Therefore, the amplitude ratio of negative-sequence current to positive-sequence current is defined to be proportional to the voltage unbalance, as expressed by

$$\frac{I_{sn}}{I_{sp}} = \frac{V_{sn}}{V_{sp}} = K_{VUF}. \quad (13)$$

The value  $I_{sp}$  is the amplitude of the positive-sequence current, which is regulated by the average power control loop. Consequently,  $I_{sn}$  is derived from (13) based on the quantity of unbalance voltage at the POC. It should be

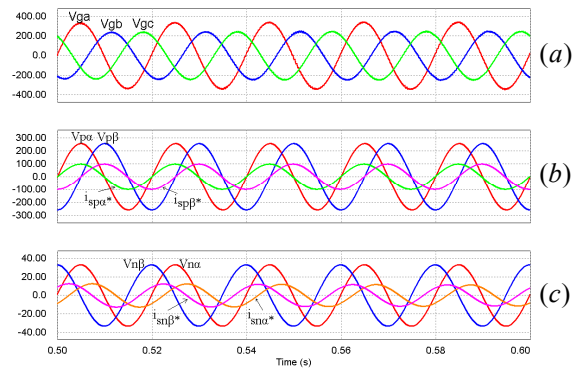


Fig. 7. Simulation results of the reference current generation. (a) unbalanced grid voltages in a-b-c frame, (b) the  $\alpha$ ,  $\beta$  components of the positive-sequence current in phase with the voltage and (c) the  $\alpha$ ,  $\beta$  components of the negative-sequence current lags the voltage by  $\varphi$  degrees in the  $\alpha$ - $\beta$  frame ( $\varphi = 45^\circ$ ).

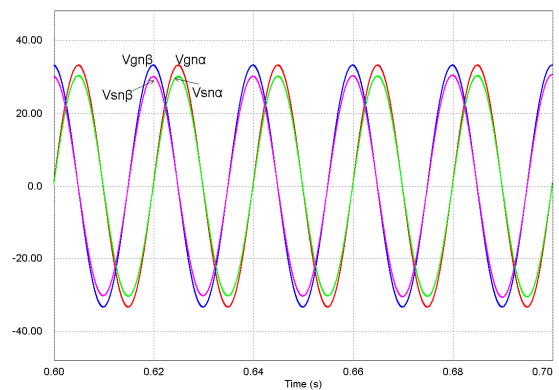


Fig. 8. Simulation results of the negative-sequence voltage correction. The  $\alpha$ ,  $\beta$  components of the negative-sequence voltage of the POC  $V_{sna,\beta}$  show a 9% of amplitude reduction comparing to the negative-sequence voltage of the grid  $V_{gna,\beta}$ .

kept in mind that the power capacity of the grid-interfacing converters is a constraint to the up limit of  $I_{sn}$ .

When this function is integrated into grid-interfacing converters, it can be regarded as an open-loop correction without a specific reference demand. As a result, the value of  $K_{VUF}$  may change back and forth when many modules operate only in the manner by injecting negative-sequence currents from (13). To ensure a stable correction, a dynamic detection is added by calculating the real-time  $K_{VUF}$  and comparing with a minimum threshold ( $K_{VUF\_min}$ ), which is defined according to practical demands. If it is above the  $K_{VUF\_min}$ , the maximum practically measured value  $K_{VUF\_max}$  will be used in (13) to get the  $I_{sn}$ . If the  $K_{VUF}$  is lower than the  $K_{VUF\_min}$ , the  $K_{VUF\_max}$  will be regulated to prevent the negative-sequence current from over-compensating.

In the average power control loop of Fig. 5, a combined proportional and integral compensator produces the current coefficient  $K_c$  to regulate the amplitudes of the desired currents. The rms value of the positive-sequence voltage is used in the loop as a feedforward to compensate for the response delay caused by average power calculation. This improves the dynamic response.

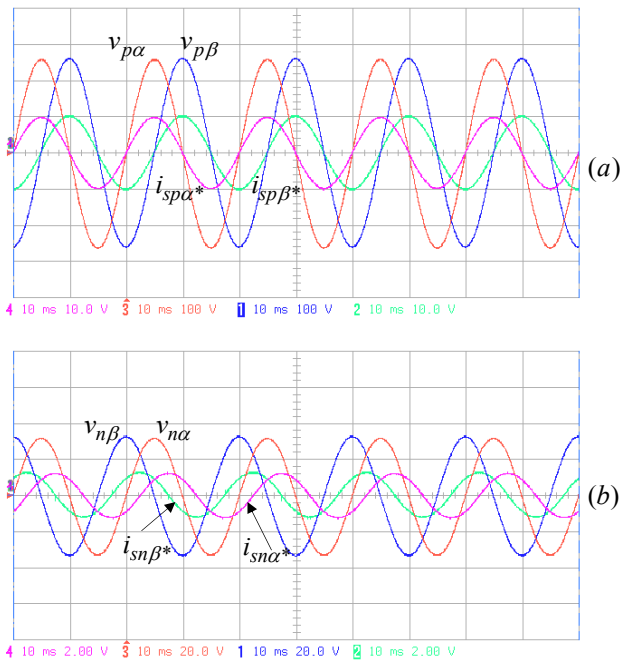


Fig. 9. Experimental results of reference current generation (a) the  $\alpha, \beta$  components of the positive-sequence current in phase with the voltage and (b) the  $\alpha, \beta$  components of the negative-sequence current lags the voltage by  $\varphi$  degrees in the  $\alpha$ - $\beta$  frame ( $\varphi = 45^\circ$ ).

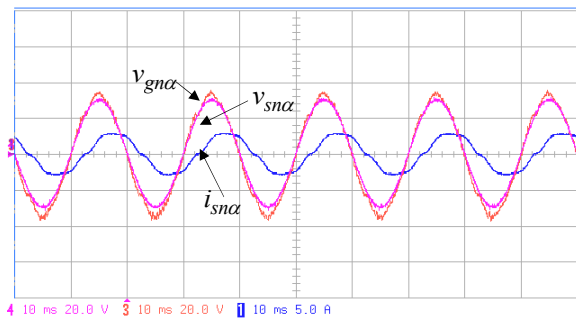


Fig. 10. Experimental results of the negative-sequence voltage correction, confirming the simulation results in Fig. 8.

It follows that the current references  $i_{s\alpha}^*$  and  $i_{s\beta}^*$  are derived in the stationary reference frame, as expressed by

$$\begin{aligned} i_{s\alpha}^* &= (i_{sp\alpha}^* + i_{sn\alpha}^*)K_c \\ i_{s\beta}^* &= (i_{sp\beta}^* + i_{sn\beta}^*)K_c \end{aligned} \quad (14)$$

In addition, the reference for zero-sequence current in the set-up of Fig. 4 should always be zero for the purpose of cancellation.

### C. Power Analysis

It is necessary to take into account the available system capacity when operating with the negative-sequence correction feature. Because the zero-sequence currents are zero, and without considering the harmonics of the grid voltage, the active power and reactive power are calculated by

$$P = \frac{3}{2}(V_{sp}I_{sp} \cos \theta_p + V_{sn}I_{sn} \cos \theta_n), \quad (15)$$

$$Q = \frac{3}{2}(V_{sp}I_{sp} \sin \theta_p + V_{sn}I_{sn} \sin \theta_n). \quad (16)$$

As already said, the angle  $\theta_p$  is designed to be zero. Hence, the reactive power is induced by the negative-

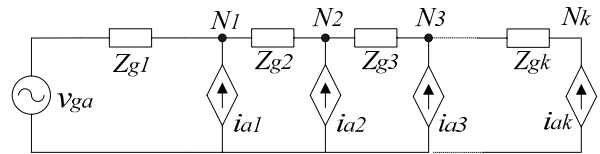


Fig. 11. Per-phase equivalent circuit of multiple modules

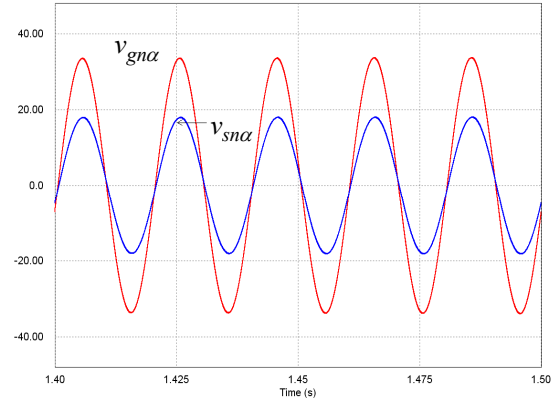


Fig. 12. Simulation results of the negative-sequence voltage at node  $N_1$  when corrected by six modules, showing in the  $\alpha$ - $\beta$  frame that the negative-sequence voltage of the grid  $V_{gn\alpha}$  has a 50% of amplitude reduction at the node  $N_1$ .

sequence component. Substituting equation (13) into (15) yields

$$P = \frac{3}{2}(1 + K_{VUF}^2 \cos \theta_n)I_{sp}V_{sp}. \quad (17)$$

This indicates that when  $\theta_n$  is not  $90^\circ$  a certain amount of active power is also required for the negative-sequence voltage correction. This extra capacity demand should always be considered in the practical application.

## 4. Simulation and Experimental Results

TABLE I – System Parameters

Description	Symbol	Value
Utility grid voltage	$V_{ga}$	$325V_{peak} / 0^\circ$
	$V_{gb}$	$225V_{peak} / 240^\circ$
	$V_{gc}$	$225V_{peak} / 120^\circ$
Line resistance	$R_g$	$0.628 \Omega$
Line inductance	$L_g$	2mH
System capacity	S	15kVA
Pos.-seq. voltage phase shift	$\theta_p$	$0^\circ$
Neg.-seq. voltage phase shift	$\theta_n$	$-45^\circ$
Orthogonal filter parameter	$\omega_b$	30 rad/s
	$\omega_1$	314 rad/s

To verify the proposed additional function and the performance of reference signals generation, the control scheme has been simulated in PSIM7.0. The system parameters are listed in TABLE I. In order to easily observe the effects of negative-sequence correction on a laboratory prototype, we intentionally exaggerate the line impedance. According to the values of line impedances in the table,  $\varphi$  should be  $45^\circ$ .

Fig. 7 shows the simulation results of the unbalanced voltage decomposition by the orthogonal filters and the generated positive-, negative-sequence references with

the PLLs. As shown in Fig. 7(b) and (c), the decomposed positive-sequence and negative-sequence reference currents in the  $\alpha$ - $\beta$  frame are presented.

With the proposed negative-sequence voltage correction added, Fig. 8 shows the effect of negative-sequence voltage correction at the POC with a single system module. As seen, the amplitude of the negative-sequence voltage is reduced, although the decrease is limited to 9%. Note that the line impedance parameters are exaggerated here for analysis. In practical utility grid, taking 200 $\mu$ H as an example, then the decrease is around 1% under the same condition.

To verify the proposal and its practical implementation, the corresponding experiment is carried out in a laboratory set-up that has the same system parameters as in the simulation. A 15KVA three-phase programmable AC power source (SPITZENBERGER+SPIES DM 15000/PAS) is used to simulate the unbalanced utility grid. The controllers are designed with dSPACE DS1104. To observe the reference signals in the  $\alpha$ - $\beta$  frame, the related waveforms have to be regenerated through D/A converters for observing. Fig. 9(a) and (b) show the regenerated reference waveforms in the practical controller, which show the same results as in simulation.

The negative-sequence voltage correction is shown in Fig. 10 by representing only  $\alpha$  components of the three-phase voltages and the negative-sequence current in the  $\alpha$ - $\beta$  frame, since the  $\beta$  components are the same except for 90° phase shift. For easier observation of the correction effects in the experiment, a simplified test was carried out. Only negative-sequence voltages were programmed at the POC, and thus a pure negative-sequence voltage correction was tested. The distortion of the current is caused by the dead-time effects, and looks notable when the outputs are very low.

As a further investigation based on the above described single module, an equivalent circuit is used to investigate correction by multiple modules in simulation. Fig. 11 shows the per-phase diagram. Many modules are distributed to different nodes on the distribution bus. For simplification, the grid-interfacing systems are replaced by current sources that assumed to deliver the same steady-state currents. The impedance may be different between every two nodes, but the ratio R/X of conductors is the same. This determines the phase angle of the reference current signals. Here all the impedances are defined to be the same value. The amplitudes of the currents at different nodes are dependant on the capacity of the system. It can be assumed that each node has the same negative-sequence current proportional to the positive-sequence current. Fig. 12 shows that the amplitude of the negative-sequence voltage corrected by six modules decreases substantially at node N<sub>1</sub>. While the effect of the correction declines gradually at the other nodes, by increasing the number of nodes in this circuit, the final result will still be substantial.

## 5. Conclusion

This paper proposes to add negative-sequence voltage correction in grid-interfacing converters. Each system module can be designed to help decrease the negative-sequence voltage at the POC. Based on the voltage unbalance factor and system capacity, the system delivers a small amount of negative-sequence current to correct the negative-sequence voltage. An experimental three-phase grid-interfacing system is employed to test this functionality and the proposed control scheme. Simulations and experiments were carried out to verify the correct operation for a single module. It can be seen that the amplitude reduction of the negative-sequence voltage is limited. However, by using many of these modules a substantial improvement is possible, as verified in an equivalent circuit by simulation.

## References

- [1] Annette von Jouanne and Basudeb (Ben) Banerjee, "Assessment of voltage unbalance," *IEEE Trans. Power Del.*, vol. 16, no. 4, pp. 782-790, Oct. 2001.
- [2] Kuang Li, Jinjun Liu, Zhaoan Wang, and Biao Wei, "Strategies and operating point optimization of STATCOM control for voltage unbalance mitigation in three-phase three-wire systems," *IEEE Trans. Power Del.*, vol. 22, no. 1, pp. 413-422, Jan. 2007.
- [3] Hideaki Fujita, and H. Akagi, "Voltage-regulation performance of a shunt active filter intended for installation on a power distribution system," *IEEE Trans. Power Electron.*, vol. 22, no.3, pp. 1046 – 1053, May 2007.
- [4] Kalyan K. Sen, "SSSC-static synchronous series compensator theory, modeling, and application," *IEEE Trans. Power Del.*, vol. 13, no. 1, pp. 241-246, Jan. 1998.
- [5] L. Gyugyi, "Unified power-flow control concept for flexible AC transmission systems," *IEE Proc.*, vol. 139, no. 4, pp. 323-331, Jul. 1992.
- [6] Vijay B. Bhavaraju and Prasad N. Enjeti, "An active line conditioner to balance voltages in a three-phase system," *IEEE Trans. Ind. Applicat.*, vol. 32, no. 2, pp. 287-292, Mar./Apr. 1996.
- [7] Milan Prodanovic and Timothy C. Green, "Control and filter design of three-phase inverters for high power quality grid connection," *IEEE Trans. Power Electron.*, vol. 18, no. 1, pp. 373-380, Jan. 2003.
- [8] Hong-seok Song and Kwanghee Nam, "Dual current control scheme for PWM converter under unbalanced input voltage conditions," *IEEE Trans. Ind. Electron.*, vol. 46, no. 5, pp. 953-959, Oct. 1999.
- [9] Sergio Augusto Oliveira da Silva, etc. "A three-phase line-interactive ups system implementation with series-parallel active power –line conditioning capabilities," *IEEE Trans. Ind. Applicat.*, vol. 38, no. 6, pp. 1581-1590, Nov./Dec. 2002.
- [10] Patricio Salmeron and Reyes S.Herrera, "Distorted and unbalanced systems compensation within instantaneous reactive power framework," *IEEE Trans. Power Del.* Vol. 22, no. 3, pp. 1655-1662, July 2006.
- [11] P.M. Andersson, Analysis of Faulted Power Systems. New York: *IEEE Press*, 1995.
- [12] H. Tao, A. Kotsopoulos, J. L. Duarte, and M. A. M. Hendrix, "A soft-switched three-port bidirectional converter for fuel cell and supercapacitor applications," in *Proc. IEEE Power Electronics Specialists Conf. (PESC'05)*, June 2005, Recife, Brazil, pp.2487-2493.
- [13] M. C. Benhabib and S. Saadate, "A new robust experimentally validated phase locked loop for power electronic control," *European Power Elec-tronics and Drives Journal*, vol. 15, no. 3, pp. 36-48, Aug. 2005.